

SOLAR ACTIVITIES AND SPACE WEATHER HAZARDS

AHMED A. HADY

*Department of Astronomy & Space and Meteorology Faculty of Sciences
Cairo University, Giza, Egypt
ahady@cu.edu.eg*

Geomagnetic storms have a good correlation with solar activity and solar radiation variability. Many proton events and geomagnetic storms have occurred during solar cycles 21, 22, and 23. The solar activities during the last three cycles, gave us a good indication of the climatic change and its behavior during the 21st century. High energetic eruptive flares were recorded during the decline phase of the last three solar cycles. The appearances of the second peak on the decline phase of solar cycles have been detected. Halloween storms during Nov. 2003 and its effects on the geomagnetic storms have been studied analytically. The data of amplitude and phase of most common indicators of geomagnetic activities during solar cycle 23 have been analyzed.

Keywords: Solar activities – solar cycles; Troposphere Halloween storm; Geomagnetic Activities.

1. Introduction

One of the most important solar phenomena is the evidence of solar activity, which has been found to be periodic with an around 11 year cycle. The occurrence of the cycle is a magnetic phenomenon, related to the dynamo effect, which generates the magnetic field of the sun (Zeldovich, et al 1983). The energetic solar events, which are associated with peak and decline phase of the solar cycles, can affect earth's atmosphere, satellites, and humankind activity. The solar cycle is important because it determines the long term variation of regions such as the earth's ionosphere, a layer of charged particles between 100 and 600 km above the surface of the earth. This layer is important because of its effect on radio signals, either reflecting high frequency signals or retarding those above this frequency range. The solar cycle also underpins the occurrence of short term disturbances to the earth-sun region. These arise in association with spectacular events on the sun such as solar flares and coronal mass ejections and propagate to the earth as changes in the solar wind, an outflow of charged particles from the sun which envelopes the earth. Disturbances disrupt the ionosphere causing rapid variations in its properties and are most obviously seen in the rapid variations in the magnetic field of the earth, events that are known as "geomagnetic storms".

A geomagnetic storm is a temporary disturbance of the Earth's magnetosphere caused by a disturbance in space

weather. Associated with solar coronal mass ejections (CME), coronal holes, or solar flares, a geomagnetic storm is caused by a solar wind shock wave that typically strikes the Earth's magnetic field 24 to 36 hours after the event. This only happens if the shock wave travels in a direction toward Earth. The solar wind pressure on the magnetosphere will increase or decrease depending on the Sun's activity. These solar wind pressure changes modify the electric currents in the ionosphere. Magnetic storms usually last 24 to 48 hours, but some may last for many days.

The energetic solar events, especially during the decline of solar cycles, can affect on earth's atmosphere, satellites, and on humankind activity. Recently, observations revealed that the solar energetic particles (SEPs) and coronal mass ejections (CMEs) with different origins, were based on magnetic changes of the active region which produced the SEPs, and on the abundances, ionization states and time production of the particles as well as the longitude distribution associations of the events, see for example: Reames, D.V. (1994) and Reames, D.V (1995). These events (SEPs and CMEs) led to severe effects on the Earth, such as power blackouts, disruption of communications, and damage of satellites.

It is well known that solar activity exhibits an 11-year periodicity, and the more dramatic activities usually occur in the maximum of the cycle. The complicated dynamics of magnetic fields play a key role in the solar activities see Parker (2001). The peak of the Solar cycle

21 was in 1979 but high energetic Solar flares, or secondary peaks, occurred at the declining phase in 1981, 1982, and 1984 before the solar activity minimum in 1986. Also, the peak of the solar cycle 22 was in 1989 but high energetic solar flares occurred at the declining phase in 1991, 1992, and 1994, before the solar activity minimum in 1996. Then the secondary peaks occurred during 2 to 3 years after the first peak, as deduced from the last five solar cycles. See for example Shaltout (1995), and Hady (2002). If a Coronal Mass Ejections (CMEs) hit the Earth, it can excite a geomagnetic storm. Large geomagnetic storms, among other things, can cause electrical power, which can damage satellite communications. In space CME typically drive shock waves that produce energetic particles that can damage both electronic equipment and astronauts that are outside the protection of the Earth's magnetic field. So, the predictions of the high energetic particle events are of vital importance for space navigation and airline safety. Shaltout et al (1996), Shaltout and Hady (2001) studied these severe effects.

1. Data analysis and Discussion

Table (1) show the data of proton flux , x-ray and optical flares , the active regions and its location in the sun disk, for the most eruptive events during the peaks and decline phase of solar cycles 21, 22 and 23. The selected proton flux , that which more than 1000 pfu (particle Flux unit), for x-ray flares the selected one which has class of x1 and more, and for optical flares of class 1f and more. The Proton fluxes are integral 5-minute averages for energies > 10 MeV, given in 9pfu), measured by GOES spacecraft at Geo-synchronous orbit: 1 pfu = 1 p/sq. cm-s-sr. SWO defines the start of a proton event to be the first of 3 consecutive data points with fluxes greater than or equal to 10 pfu. The end of an event is the last time the flux was greater than or equal to 10 pfu.

From the table (1), we can note that:

1. Through the decline of the current solar cycle 23, there are sudden rises with the solar activates. During the period from 28 October to 4 November 2003, there was a sudden and high solar activity in the active region Number 10486, and produced one of the most eruptive flare recorded since 1976.

2. During the period from 28 October to 4 November 2003, the proton flux reached 29500 pfu. The x-ray flare to X17, and reached to X28 in 4 November 2003. While optical flares are 4B and reached to 3B at 4 November 2003. The x -ray sensors on-board the GOES spacecraft are not capable of registering x-ray intensities up to level of class. It appears that this x-ray flare peaked somewhere between the X30 and X40 class level.

The X-ray classification of solar flares is a most useful measure of the strength of a flare. To classify the most energetic flares since 1976, we will use a usual classification of fares, by descriptive letter M if the X-Ray power output is in the range of 0.01 to 0.1 ergs/square centimeter/second and the letter X if it is above a value of 0.1.

Table 1: Eruptive solar proton events, and eruptive Flares affecting the Earth environment, During the Peaks and declining phases of the solar cycles 21, 22 and 23

-----Proton Flux-----			-----Flares-----		
Start Date/UT	Max. Proton Flux (pfu@>10 MeV)	Flare Max. Importance	Flare Date/UT	Max. Importance X-ray/Opt. Loc.	Region No.
(Peak of Cycle 21)					
19780923/1035	0924/0400	2200	0923/1023	X1/3B	N35W50 1294
(decline of Cycle 21)					
19811008/1235	1013/2247	2000	1007/2308	X3/1E	S19E88 3390
19820711/0700	0713/1615	2900	0709/0742	X9/3E	N17E73 3804
19821208/0010	1208/1000	1000	1207/2354	X2/0E	S14W81 4007
19840425/1330	0426/1420	2500	0425/0005	X13/3E	S12E43 4474
(Peak of Cycle 22)					
19890308/1735	03 3/0645	3500	0306/1405	X15/3E	N35E69 5395
19890317/1855	0318/0920	2000	0317/1744	X6/2E	N33W60 5395
19890812/1600	0813/0710	9200	0812/1427	X2/2E	S16W37 5629
19890929/1205	0930/0210	4500	0929/1133	X9/EPL	S26W90 5698
19891019/1305	1020/1600	40000	1019/1258	X13/4B	S27E10 5747
19891130/1345	1201/1340	7300	1130/1229	X2/3E	N26W59 5800
(decline of Cycle 22)					
19910323/0820	0324/0350	43000	0322/2247	X9/3E	S26E28 6555
19910604/0820	0611/1420	3000	0604/0352	X12/3B	N30E70 6659
19910614/2340	0615/1950	1400	0615/0821	X12/3B	N33W69 6659
19910707/0455	0708/1645	2300	0707/0223	X1/2E	N26E03 6703
19940220/0300	0221/0900	10000	0220/0141	M4/3E	N09W02 7671
(Peak of Cycle 23)					
20000714/1045	0715/1230	24000	0714/1024	X5/3E	N22/W07 9077
20001108/2350	1109/1600	14800	1108/2328	H7/mult	N00-10 9213
20010924/1215	0925/2235	12900	0924/1038	X2/2E	W75-80 9213
20011104/1705	1106/0215	31700	1104/1620	X1/3E	S16E23 9632
20011122/2320	1124/0555	18900	1122/2330	H9/2N	N06W18 9684
(decline of Cycle 23)					
20020421/0225	0421/2320	2520	0421/0151	X1/1F	S14W8 9906
20031028/1215	1029/0615	29500	1028/1110	X17/4B	S16E08 10486
20031102/1105	1103/0815	1570			
20031104/2225	1105/0600	353	1104/1915	X28/3b	S19W83 10486

A multiplier number is also attached to the description so that an X5.0 flare has a power of 0.5 ergs/square centimeter/second. Class M flares, particularly the less energetic ones, are likely to cause a fadeout on the lowest frequencies of the High Frequency (HF) radio spectrum. On the other hand X class flares will cause a fadeout for all HF frequencies over the entire day light hemisphere of the earth. Class X flares are also more likely to be associated with a host of interesting effects here on earth and in space. It is the Class X flares which are of greatest interest to those affected by the sun, for more details see Richard Thompson (2004).

Table(2), the daily Geomagnetic data of the Most eruptive days during the Peak period and decline period of Solar cycle 23 . Fredericksburg, College, and Estimated Planetary A and K Indices, were tabulated. The daily 24-hour A index and eight 3-hourly K indices from the Fredericksburg (middle-latitude) and College

(high-latitude) stations monitoring Earth's magnetic field. The estimated planetary 24 hour A index and eight 3-hourly K indices are derived in real time from a network of western hemisphere ground-based magnetometers.

From this table, geomagnetic data show dramatic increases of recorded values during October – November 2003, compared with data during the period

Table 2: Daily Geomagnetic data of most robust eruptive days during the Peak and declining phase of solar cycle 23.

Date	Middle Latitude --Fredericksburg--								High Latitude ---College---								Estimated ---Planetary ---										
	A				--K-indices--				A				--K-indices--				A				--K-indices--						
20000714	33	3	3	3	3	3	6	6	4	49	4	4	3	5	4	7	6	4	35	4	3	4	4	4	6	5	4
20000715	148	3	3	3	3	6	8	9	9	-	3	4	5	6	7	-	-	152	4	4	5	5	6	9	9	9	
20001108	14	1	3	4	4	3	3	1	2	-	-	-	-	-	-	-	-	15	2	3	4	4	3	3	1	3	
20001109	10	3	1	1	1	3	3	2	3	21	2	2	1	3	5	5	4	3	11	3	1	1	1	3	3	3	
20010924	5	3	2	1	1	1	1	1	1	4	3	1	1	0	1	1	1	1	6	3	1	1	2	2	2	1	
20010925	17	1	2	2	0	3	0	4	6	23	1	2	2	0	0	6	6	18	1	2	2	1	1	2	5	6	
20011104	4	0	0	2	3	1	2	1	0	17	0	0	3	5	5	3	2	0	7	0	0	2	3	3	2	1	
20011105	12	0	0	1	2	4	3	4	3	11	0	0	0	2	3	4	4	13	0	0	1	2	3	4	5	4	
20011122	8	1	2	2	2	2	3	2	3	-	0	2	2	-	2	2	1	8	1	2	2	3	2	2	3	2	
20011123	11	2	1	2	2	3	4	1	3	23	3	2	3	4	5	5	2	12	3	2	2	2	3	3	3	3	
20020421	4	1	1	1	1	1	1	2	2	7	3	2	2	0	1	2	2	7	3	2	2	1	2	2	2	3	
20031028	15	2	4	3	3	2	3	3	3	28	2	3	5	3	5	4	3	20	3	4	4	4	3	4	3	4	
20031029	199	3	3	9	6	7	7	9	9	97	5	4	9	8	7	8	9	189	4	3	9	8	7	7	9	8	
20031030	144	7	5	4	4	6	9	9	124	6	5	4	6	7	8	7	8	162	8	7	6	5	5	8	9	9	
20031031	73	8	7	6	4	5	3	3	3	69	6	6	6	6	5	6	4	93	8	7	7	6	6	5	4	4	
20031101	16	5	4	3	1	2	2	1	3	32	4	4	5	5	5	4	3	21	4	5	4	3	3	3	3	3	
20031102	11	3	3	2	2	3	3	2	27	4	3	3	4	5	5	4	2	18	3	4	3	3	4	4	3	3	
20031103	15	4	2	1	1	5	2	2	3	12	3	3	1	3	2	3	2	10	3	3	2	3	2	3	2	3	
20031104	20	2	2	5	5	2	2	4	2	34	3	3	5	7	3	2	4	31	3	2	5	7	3	3	4	3	

of solar cycle 23. This increase has its peak during 29 November as in proton flounce case. This means those there effects of proton particle and the geomagnetic field. The data given from GOES-11 Space Environment Monitor with daily average of 5-Minots records of x-ray flux for two energy bands 1-8 Ao, 0.5-3 A° were given and tabulated in table (3).

The magnetic flux was tabulated too, where:

- XL 1-8 Ang X-ray Flux (Watts/Meter²)
- XS 0.5-3 Ang X-ray Flux (Watts/Meter²)
- Hp (parallel) Northward Magnetic Flux (nanotesla)
- He Earthward Magnetic Flux (nanotesla)
- Hn (normal) Eastward Magnetic Flux (nanotesla)
- Ht Total Magnetic Flux (nanotesla).

Table 3: X-ray flux and Magnetic flux during the most eruptive days during Peak and decline phase of the solar cycle 2.

Date /UT	-- X-ray Flux--		Magnetic Flux (Nanotesla)			
	1-8 A°	0.5-3 A°	Northward	Earthward	Eastward	Total
	XL	XS	HP	HE	HN	HT
20000714/17 00	5.13E-006	3.71E-007	169.00	35.40	2.67	172.69
20001107/19 12	1.21E-006	2.32E-008	178.00	22.60	-3.80	179.47
20010924/00 15	2.58E-006	7.05E-008	143.00	11.80	25.00	145.65
20011114/17 25	1.66E-006	2.64E-008	117.00	15.90	18.30	119.49
20011114/17 30	1.60E-006	2.43E-008	118.00	15.60	18.40	120.44
20011121/19 05	1.50E-006	2.93E-008	114.00	15.90	19.00	116.66
20020421/17 50	6.93E-006	8.77E-007	122.00	50.80	-3.91	132.21
20031028/12 15	3.27E+004	3.27E+004	327.11	327.11	327.11	327.11
20031102/11 05	3.27E+004	3.27E+004	327.11	327.11	327.11	327.11
20031104/22 25	3.27E+004	3.27E+004	327.11	327.11	327.11	327.11
20031118/01 16	3.27E+004	3.27E+004	327.11	327.11	327.11	327.11
20040101/00 00	3.24E-006	1.41E-007	110.00	11.50	22.30	112.83
20040131/22 15	1.92E-007	8.13E-009	123.00	14.00	21.80	125.70

Form this table, the on-board GOES magnetic flux sensors are not capable to register over than 327.11 Nanotesla, and the detectors was saturated. For the 4 types of measurements, during October– November 2003. It appears that this Magnetic flux peaked more than that level. The x-ray flux in the selected two bands recorders as decrease of registrations during October – November 2003. In the other hand from table (1), the proton flux reach to 29500 pfu, The x-ray flare to X17 at 28 October 2003, and reach to X28 in 4 November 2003. This means that the eruptive solar flare during October 2003 did not have any effects in these two bands only. All these eruptive and most robust solar events during solar cycle 23 decline developed and released from to active region 10486 and 10488.

Table 4: The selective data for the most eruptive days during peak and decline phase of solar cycle 23, for the Belt Indices of Relative Intensities of NOAA/POES Energetic Particles.

Date	Sensor Number	Total Belt Index	Inner Belt Index	Solar Belt Index	Outer Belt Index
20000811	3	2.1554	1.4735	1.0274	2.3749
20000924	18	3.6422	0.9232	0.9604	286.9992
20001104	18	3.1238	0.8795	0.9746	241.3332
20011122	1	0.9140	0.9730	1.0053	0.8926
20020421	5	12.6356	0.7694	2.6364	18.4204
20020421	15	8.5070	0.8951	1.2205	5743.1426
20020421	18	9.7825	0.8752	0.9982	1077.1337
20020422	5	12.1110	0.7310	5.4506	16.8909
20031020	15	0.6004	1.0507	2.3744	2110.3030
20031028	18	17.9682	1.0415	1.1323	1974.2799
20031029	13	37.5394	0.9548	119.3444	1185.9089
20031029	15	129.6573	1.1536	12.9669	41814.7930
20031029	18	56.7950	0.9721	9.5347	6490.7021
20031030	13	14.6328	0.8710	427.4738	445.4869
20031030	15	42.0337	0.8920	30.5849	9825.1104
20031031	7	20.3387	1.3570	202.2258	19.5264
20031031	9	29.5982	3.2523	343.2895	30.8484
20031101	5	11.5378	2.0870	52.2854	12.4471
20031102	5	22.7356	3.2677	140.5020	22.2892
20031102	15	2.4396	1.1205	16.6281	213.8485
20031103	15	30.7781	1.1019	16.2800	633.0806
20031104	15	26.9992	1.0651	14.6436	5195.9331

The belt indices for selective days during solar cycle 23, which have eruptive events, are given in table (4). The belt indices are a measure of the integrated difference, or departure, of individual sensor responses observed on a given day from the responses of those sensors as averaged over the previous year's observations. Just as each orbital data "point" (2x5 degree box) in the "tiger plot" of Relative Intensities of NOAA/POES Energetic Particles displays a color-coded ratio of the particle count to a one-year average particle count, the belt indices are the ratio of the whole day's summed particle counts to their corresponding one-year summed average. The indices are subdivided by the L-values of the points, resulting in three separate values, corresponding to: inner (L-value < 2.0), slot (2.0 <= L-value < 2.5), and outer (L-value >= 2.5), and finally a total index which accounts for all points, without regard to L-value.

The data of total belt index in the table have a sudden increase of its records during 29 October 2003, after one day from the eruptive flare release. The outer belt index recorded data on 29 more than 50 times as on 28 October 2003, compared with that on 20 October 2003. While in total belt index on 29 October is more than 8 times as on 28 October 2003. In solar Belt index have its maximum on 30 October for few hours only, its more than 3 time

that recorded on 29 October 2003. The sudden increase of all belts Index are due to the eruptive flare in October – November 2003, and its clear the great effects of all events related to the sun at that period of time .

2. Historical occurrences

From August 28 until September 2, 1859, numerous sunspots and solar flares were observed on the sun, the largest flare occurring on the 1st. A massive CME headed directly at Earth due to the solar flare and made it within eighteen hours—a trip that normally takes three to four days. On September 1 and 2nd, the largest recorded geomagnetic storm occurred. The horizontal intensity of geomagnetic field was reduced by 1600 nT as recorded by the Colaba observatory near Bombay, India. Telegraph wires in both the United States and Europe shorted out, some even causing fires. Auroras were seen as far south as Hawaii, Mexico, Cuba, and Italy—phenomena that are usually only seen near the poles. This was the 1859 solar super-storm.

On 13 March 1989 a severe geomagnetic storm caused the collapse of the Hydro-Québec power grid in a matter of seconds as equipment protection relays tripped in a cascading sequence of events. Six million people were left without power for nine hours, with significant economic loss. The storm even caused auroras as far south as Texas. The geomagnetic storm causing this event was itself the result of a Coronal Mass Ejection, ejected from the Sun on March 9, 1989.

In August 1989, another storm affected microchips, leading to a halt of all trading on Toronto's stock market .

Since 1989, power companies in North America, the UK, Northern Europe and elsewhere evaluated the risks of geomagnetically induced currents (GIC) and developed mitigation strategies.

Since 1995, geomagnetic storms and solar flares have been monitored from the Solar and Heliospheric Observatory (SOHO) joint-NASA-European Space Agency satellite.

On Feb. 26, 2008 the magnetic fields erupted inside the magneto tail, releasing about 1015 Joules of energy. The blast launched two gigantic clouds of protons and electrons, one toward Earth and the other away from Earth. The Earth-directed cloud crashed into the planet below, sparking vivid auroras in Canada and Alaska.

Figure 1 show the sunspot number and AA geomagnetic index correlations since 1968 until 1992.

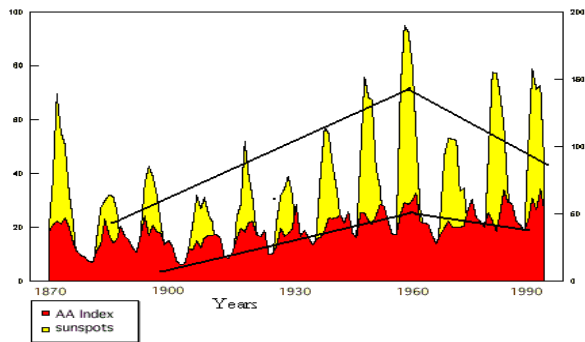


Figure 1: Sunspot number and AA index correlations since 1968 until 1992

We can see a good correlation between them and the appearance of 84-year periodicities overwhelm the 11-year solar cycle. Another geomagnetic index correlation with sunspot number (11-year solar cycle) appear in the figure (2) the A_p index since 1930 until 2000. From figure(3), of the annual average geomagnetic activity index during the solar cycle 10 until solar cycle 22 we can observe that during cycles 21, 22 the solar activity is higher than that the other cycles as shown in the figure(3). From figure(3), we can see that the solar cycle 23 has lower sunspot numbers than as in cycles 21, 22, that means the solar activity during cycle 23 the lower than that in solar cycles 21, 22.

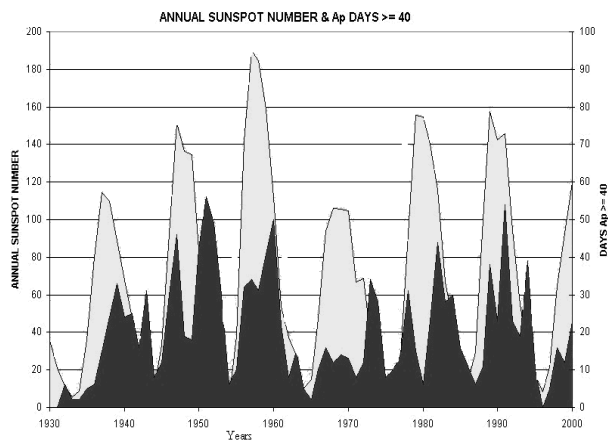


Figure 2: the A_p index and sunspot number since 1930 until 2000.

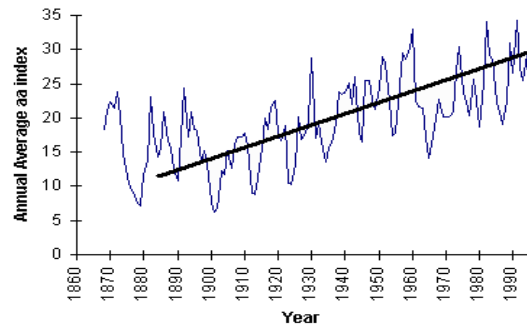


Figure 3: Annual average geomagnetic activity Index and geomagnetic index during years period, 1868-1995.

3. Interactions with planetary processes

The solar wind also carries with it the solar magnetic field. This field will have either a North or South orientation. If the solar wind has energetic bursts, contracting and expanding the magnetosphere, or if the solar wind takes a southward polarization, geomagnetic storms can follow. The southward field causes magnetic reconnection of the dayside magnetopause, rapidly injecting magnetic and particle energy into the Earth's magnetosphere.

During a geomagnetic storm, the ionosphere's F2 layer will become unstable, fragment, and may even disappear. In the Northern and Southern pole regions of the Earth, auroras (aka Northern lights) will be observable in the sky. The Magnetosphere in the near-Earth space environment shown in figure (4).

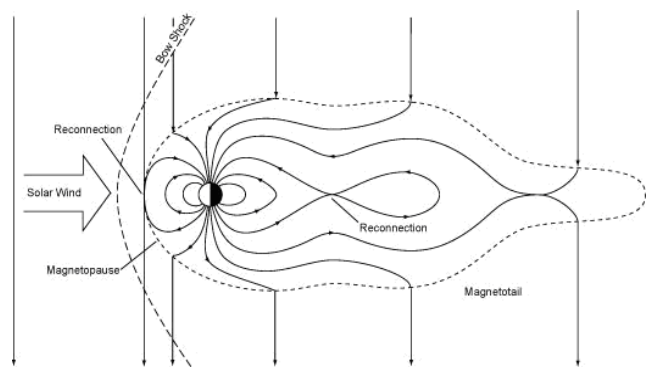


Figure 4: Magnetosphere in the near-Earth space environment

4. Geomagnetic Storm Effects

1. Radiation hazards to humans: Intense solar flares release very-high-energy particles that can cause radiation poisoning to humans in the same way as low-energy radiation from nuclear blasts. Earth's atmosphere and magnetosphere allow adequate protection at ground level, but astronauts in space are subject to potentially lethal doses of radiation. The penetration of high-energy particles into living cells can cause chromosome damage, cancer, and a host of other health problems. Large doses can be fatal immediately. Solar protons with energies greater than 30 MeV are particularly hazardous. There is a growing body of evidence that changes in the geomagnetic field affect biological systems..

2. Disrupted systems: In Communications: Many communication systems use the ionosphere to reflect radio signals over long distances. Ionospheric storms can affect radio communication at all latitudes. Some radio frequencies are absorbed and others are reflected, leading to rapidly fluctuating signals and unexpected propagation paths.

In Navigation systems: Systems such as GPS, LORAN, and the now-defunct OMEGA, are adversely affected when solar activity disrupts their signal propagation. The OMEGA system consisted of eight transmitters located throughout the world. Airplanes and ships used the very low frequency signals from these transmitters to determine their positions. During solar events and geomagnetic storms, the system gave navigators information that is inaccurate by as much as several miles.

In Satellites: Geomagnetic storms and increased solar ultraviolet emission heat Earth's upper atmosphere, causing it to expand. The heated air rises, and the density at the orbit of satellites up to about 1000 km increases significantly. This results in increased drag on satellites in space, causing them to slow and change orbit slightly. Unless Low Earth Orbit satellites are routinely boosted to higher orbits, they slowly fall, and eventually burn up in Earth's atmosphere.

5. Conclusion

1. Solar particle events (SPEs) with very high fluxes of solar protons have correlation with geomagnetic storms.
2. Geomagnetic Indices (A and K indices) increased with increasing solar activities with time delay of one to two days.
3. Solar activity is a direct result of the solar dynamo sustained by the differential rotation and turbulent convection.

4. Solar activity affects solar irradiance. Solar activity results in coronal holes with open magnetic fields that produce fast solar wind.

5. Closed-field regions produce CMEs and flares that have serious space weather consequences, SEPs and geomagnetic storms.

References

1. Hady A., Planetary and space science 50, 2002, pp89-92, (2002).
2. Hady A., Shaltout M. A., European Geo-sciences Union 2004, General Assembly 2004, Vol. 6 ,2004, p00195. (2004).
3. Krivski L., Bolleten of Astronomical Institute of Czechoslovakia, vol. 26, No. 4, 203, (1975).
4. Michalek G., N. Gopalswamy, A. Lara and P.K. Manoharan, European Geosciences Union 2004, General Assembly 2004, Vol. 6, 02819, (2004).
5. Mininni P. D., Gomez, D. O. and Mindline G. B., solar physics Rev. Lett. 85, 5476, (2000).
6. Parker E. N., Chin. J. Astron. Astrophys., 1, 99, <http://www.chjaa.org> (2001).
7. Pontieri A., F. Lepreti, L. Sorriso-Volvo, A. Vecchio and V. Carbone, Solar physics 213, pp195-201, (2003).
8. Reames, D.V., Meyer, J.P., and von Roseninge, T. T., Astrophys. J. Suppl. 90, 1994, 649.
9. Reames, D.V., Revs. Geophys (Suppl.) 33, p585 (1995).
10. Richard Thompson, Copyright IPS- Radio and Space Services, (2002). <http://www.noaa.gov/index.html/>
11. Robert Erdelyi, European Geosciences Union 2004, General Assembly 2004, Vol. 6, p06293 (2004).
12. Shaltout M. S. and Hady Ahmed A, IAGA-IASPEI, Joint scientific Assembly, 19-31 August 2001, Hanoi, Vietnam, (2001).
13. Viereck and Puga, JGR, 104, pp9995-10005, (1999)
14. Viereck and Puga, "The Mg II Index: A proxy for Solar EUV". GRL, 28, April (2001). 2-001, pp1343-1346, (2001).
15. Zeldovich, Ya. B., Ruzmaikin, A. A., and Sokoloff, D. D. "Magnetic field in astrophysics" Golden and Breach Sciences Publishers, 1983, New York, (1983).